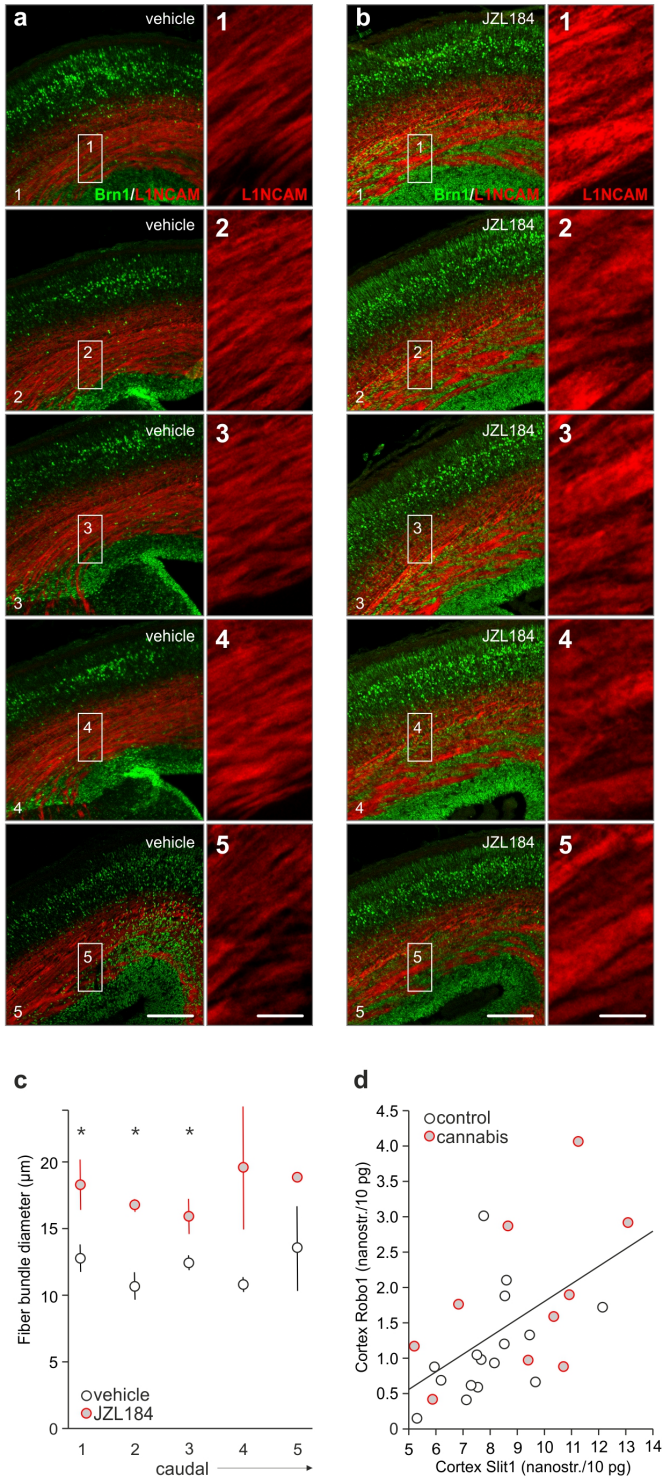

Supplementary Figure 1 | JZL184 administration alters axon fasciculation.

(**a,b**) L1-NCAM^{+} axons in the corpus callosum of JZL184- or vehicle-treated mouse fetuses at different rostro-caudal levels including the anterior commissure (1), the rostral pole of the hippocampus (5) and intermediate levels (2-4). (**c**) The diameter of axon fascicles in the corpus callosum, as shown for every corresponding coordinate (*$p < 0.05$). (**d**) Cortical Robo1 mRNA expression in cannabis-exposed human fetal subjects. Similarly for Slit1, there was a significant confound of development resulting in only a weak trend effect ($p = 0.093$) for the contribution of cannabis exposure. Data were expressed as means ± s.e.m., $n = 4$ – 6 mouse embryos/group; *$p < 0.05$ (Student's *t*-test). *Scale bars* = 200 µm (a,b), 10 µm (enumerated insets).

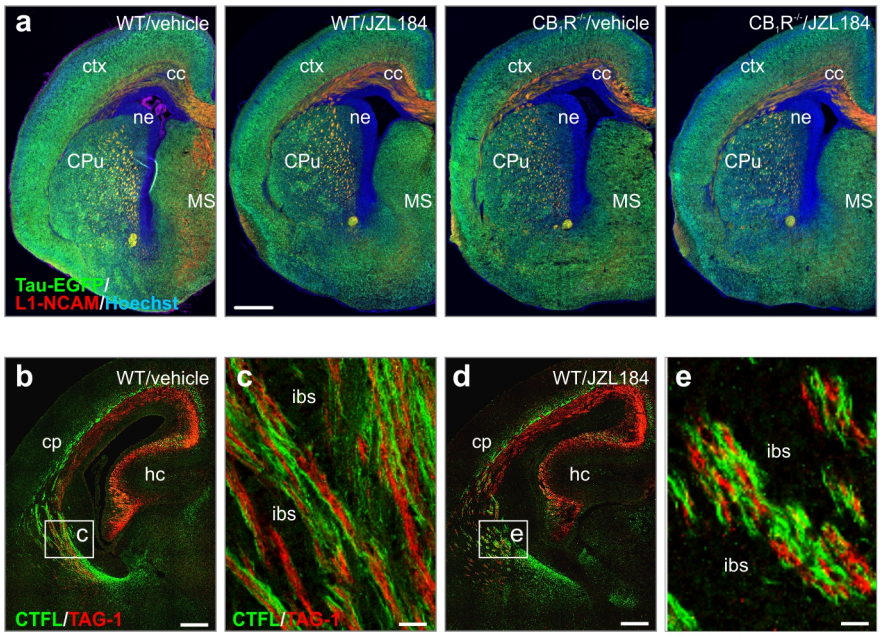

Supplementary Figure 2 | The lack of CB_1Rs or exposure to JZL184 modulates axon fasciculation in the fetal brain.

(**a**) Overview images showing enlarged callosal axon bundles in the absence of CB_1Rs in mice with GFP-tagged cytosolic tau ubiquitously expressed by cortical pyramidal neurons[17]. Note that subcortical neurons are also GFP-labeled. JZL184 did not alter the pattern of GFP expression. (**b-e**) JZL184 exposure during late gestation triggers coincident changes in CB_1R^+ cortithalamic axons and CB_1R^- thalamocortical afferents[18] during their reciprocal pathfinding (termed as "handshake")[19]. Note the increased inter-bundle space (ibs) amongst axon fascicles coursing at the pallio-subpallial boundary (**c,e**). TAG-1 is a neural cell adhesion molecule expressed in the corticofugal system[16,20]. CTFL ("*C-terminal flanking epitope*") is a recently described pan-histochemical marker for thalamocortical axons[14]. *Scale bars* = 200 µm (a,b,d), 5 µm (c,e).

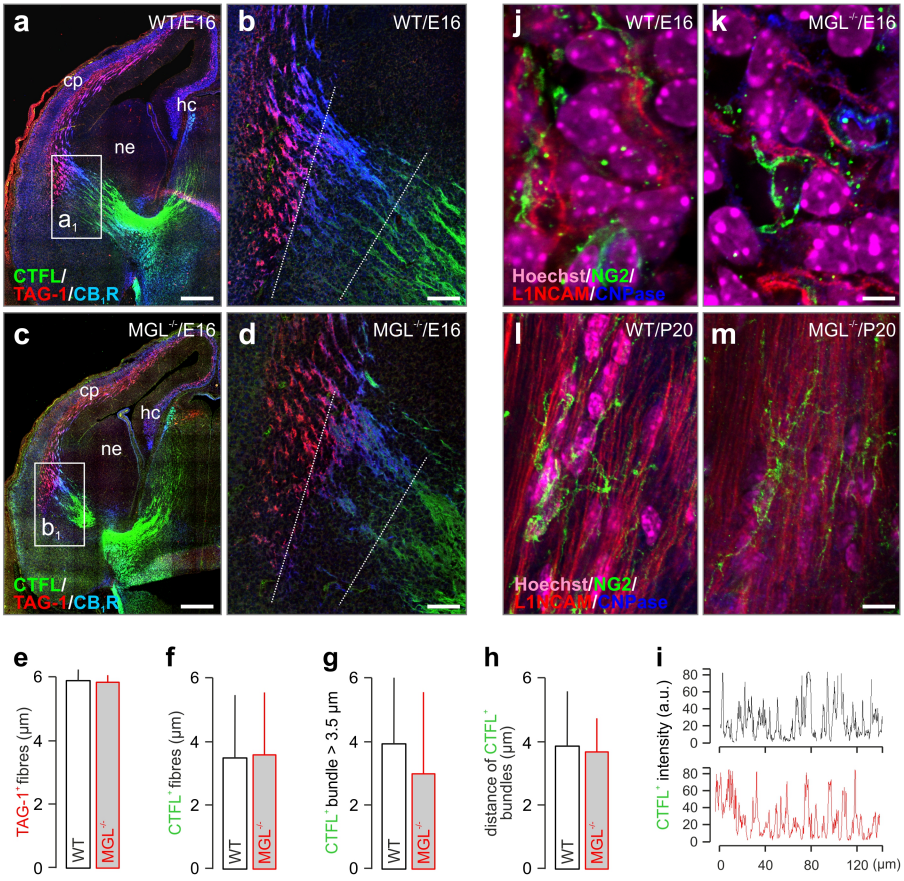

Supplementary Figure 3 | Constitutive MGL$^{-/-}$ mice develop without axon fasciculation defects or premature oligodendrogliogenesis.

(**a-d**) The corticofugal system of MGL$^{-/-}$ embryos develops normally with no overt effect of MGL deletion on the fasciculation (**e,f**), distribution (**g,h**) or labeling intensity (**i**) of thalamocortical axons revealed by CTFL ("*C-terminal flanking epitope*"), a pan-histochemical marker of these afferents[14]. Fluorescence intensity plots (**i**) were calculated along the trajectories shown by dashed lines in (**b**) and (**d**). (**j,k**) Developmentally premature CNPase^{+} or NG2^{+} oligodendrocyte proliferation or overt oligodendrocyte accumulation in adulthood (**l,m**) were equally absent in MGL$^{-/-}$ mice, as compared to wild-type littermates. Data were expressed as means ± s.e.m.; *n* = 3-4/genotype. *Scale bars* = 200 µm (a,c), 15 µm (b,d), 5 µm (k,m).

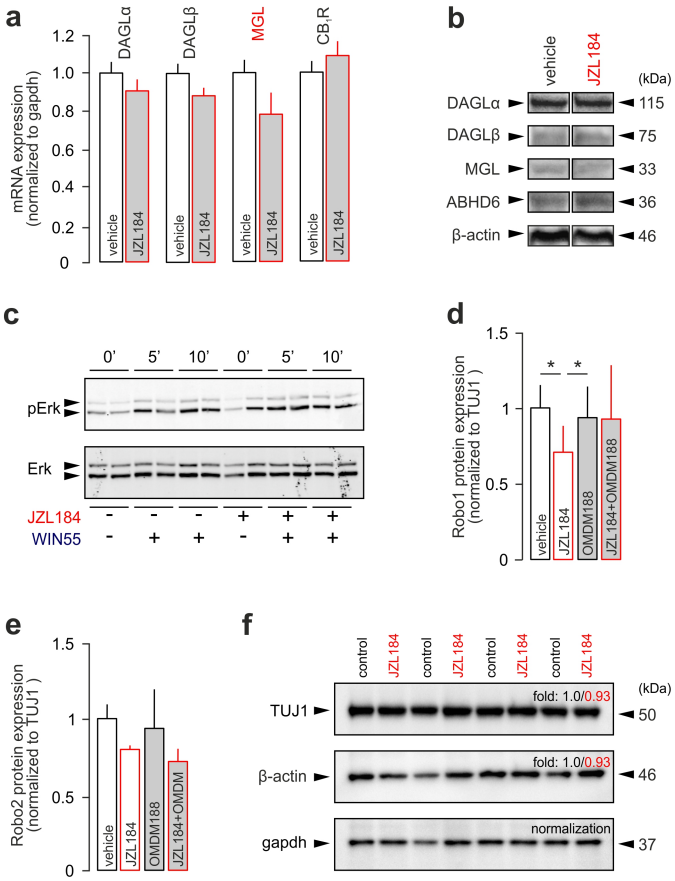

Supplementary Figure 4 | Downstream effects of JZL184 *in vivo*.

(**a**) Maternal JZL184 treatment did not affect mRNAs of DAGLα, DAGLβ, MGL and CB_1Rs in mouse embryonic cortices. (**b**) Western blot images showing protein expression levels of enzymes involved in 2-AG metabolism (quantitative analysis is shown in **Fig. 2s**). (**c**) Erk1/2 phosphorylation after acute WIN55,212-2 treatment of cultured cortical neurons in control or after exposure to JZL184 for 4 days. (**d,e**) Robo1 and Robo2 protein levels in cultured cortical neurons treated with JZL184 alone or in combination with the DAGLα inhibitor OMDM188[21]. Data were normalized to β-III-tubulin (TUJ1) as loading control. (**f**) Total amounts of the cytoskeletal markers TUJ1 and β-actin, normalized to glyceraldehyde-3-phosphate dehydrogenase (gapdh), upon exposure of cultured cortical neurons to JZL184 or vehicle. Data were expressed as means ± s.e.m. Experiments were performed in triplicate with $n \geq 2$ samples processed in parallel. $*p < 0.05$ (Student's *t*-test).

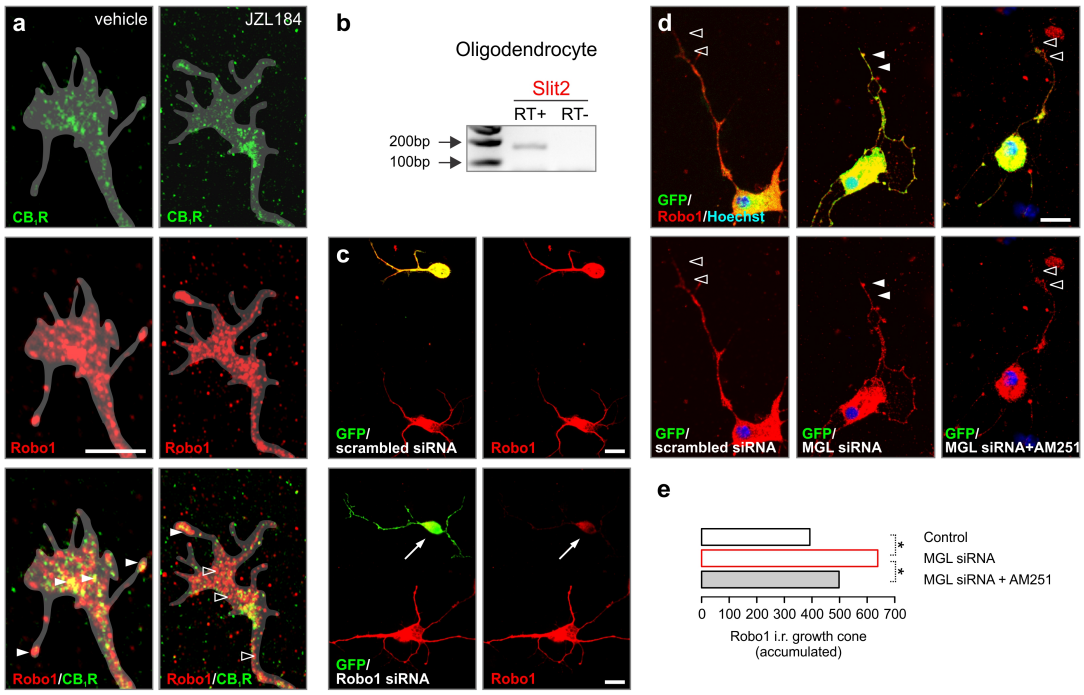

Supplementary Figure 5 | Robo1 manipulation in cultured neurons.

(**a**) Co-localization of CB_1R and Robo1 immunoreactivity in growth cones in vehicle and JZL184-treated mouse neurons. (**b**) Slit2 mRNA transcripts in cultured oligodendrocytes. (**c**) Robo1 immunoreactivity in neurons co-transfected with Robo1 siRNA and GFP relative to that in neurons co-transfected with scrambled siRNA and GFP. (**d,e**) Cortical primary neurons co-transfected with MGL siRNA showed increased Robo1 immunoreactivity within the growth cone. Data in (**e**) were expressed as means ± s.e.m., n = 6-8/group; *$p < 0.05$ (Student's t-test). *Scale bars* = 20 µm (d), 10 µm (**c**), 3 µm (**a**).

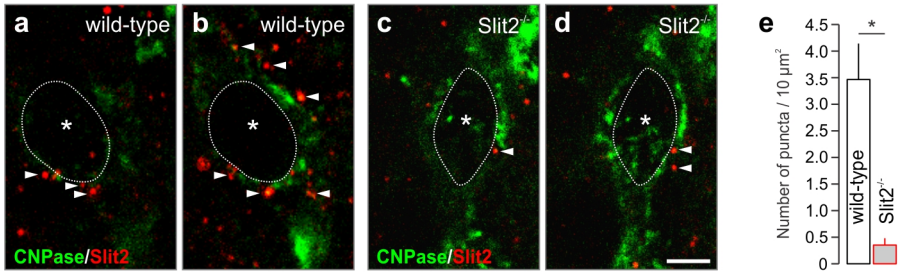

Supplementary Figure 6 | Slit2 antibody validation in oligodendrocytes of Slit2$^{-/-}$ mice.

(**a-b**) Slit2^{+} puncta (*arrowheads*) associated with CNPase^{+} oligodendrocyte somas (*asterisks*) and end-feet as imaged in 600 nm-thin serial optical sections. Genetic deletion of Slit2^{22} abolished Slit2 immunoreactivity localized to oligodendrocytes (**c-e**). Data were expressed as means ± s.e.m., n = 2 animals/genotype; $n \geq 5$ images/animal; *$p < 0.05$ (Student's t-test). *Scale bars* = 10 µm (d).

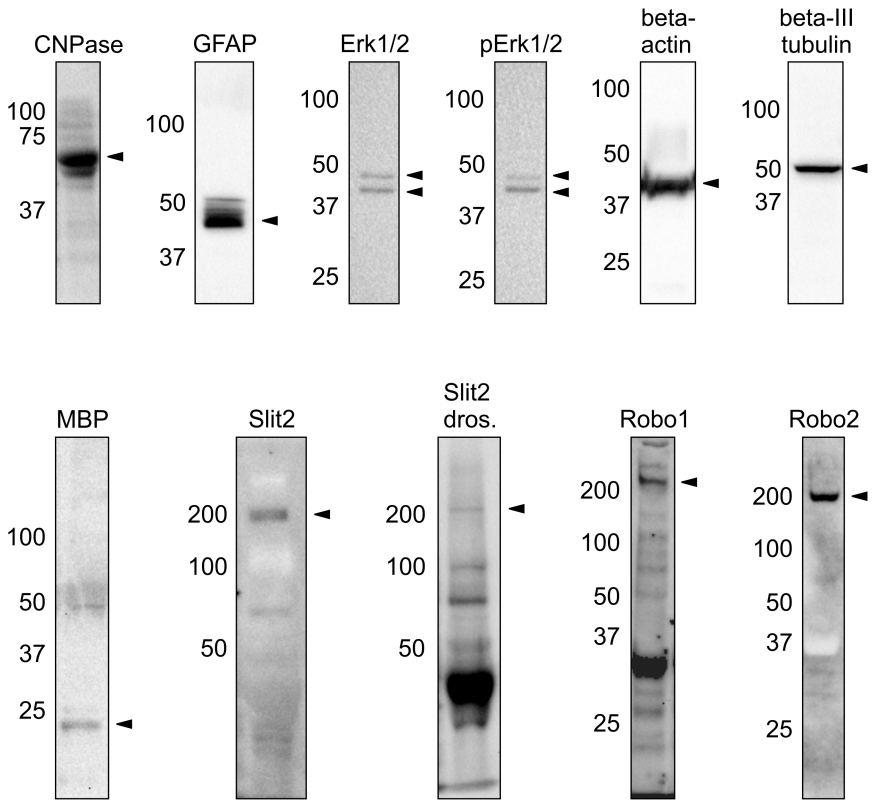

Supplementary Figure 7 | Staining profiles of antibodies used in this study.

Full-length Western blotting staining profiles of antibodies used in this study. Arrowheads point to bands of expected size. Molecular weight markers in kDa.

Supplementary Table I | List of markers used for immunofluorescence labeling.

Panel of antibodies used in this study. Staining methods and antibody specificities were described in detail elsewhere[1-16]. *Abbreviations:* IH, immunohistochemistry; WB, Western blotting.

Marker	Source	Host	IH dilution	WB dilution	Reference
Brn-1	Santa Cruz	Goat, pc[2]	1:500	1:50	Keays *et al.* (2007)
CB_1R	Dr. M. Watanabe	Goat, pc[2]	1:1,000	n.a.	Keimpema *et al.* (2013)
CNPase	Sigma	Mouse, mc[1]	1:500	1:1,000	Kasama-Yosida *et al.* (1997)
CTFL	Santa Cruz	Rabbit, pc[2]	1:1,000	n.a.	Wu *et al.* (2010)
DAGLα	Dr. K. Mackie	Rabbit, pc[2]	1:500	1:500	Mulder *et al.* (2011)
DAGLβ	Dr. K. Mackie	Rabbit, pc[2]	1:500	1:500	Mulder *et al.* (2011)
GAP-43	Millipore	Mouse, mc[1]	n.a.	1:1,000	Benowitz & Routtenberg (1997)
GFAP	Synaptic Systems	Guinea Pig, pc[2]	1:800	1:2,000	Antonucci *et al.* (2012)
L1-NCAM	Millipore	Rat, pc[2]	1:2,000	n.a.	Lopez-Bendito *et al.* (2006)
MBP	Boehringer Mannheim	Mouse, mc[1]	n.a.	1:1,000	Bologa *et al.* (1986)
MGL	Dr. K. Mackie	Rabbit, pc[2]	1:500	1:1,000	Mulder *et al.* (2011)
Neurocan	R&D Systems	Sheep, oc[2]	1:20	n.a.	Bekku & Oohashi (2010)
NG2	Millipore	Rabbit, pc[2]	1:200	n.a.	Zhao *et al.* (2006)
RC2	Millipore	Mouse, mc (IgM)[1]	1:250	n.a.	Mulder *et al*. (2008)
Robo1	Dr. F. Murakami	Rabbit, pc[2]	2.5mg/ml	10mg/ml	Andrews *et al.* (2006)
Robo2	Dr. F. Murakami	Rabbit, pc[2]	8.3mg/ml	15mg/ml	Andrews *et al.* (2006)
Slit (Drosophila, C555.6)	Hybridoma Bank	Mouse, mc[1]	n.a.	1:100	Rothberg *et al.* (1990)
Slit2	Millipore	Rabbit, pc[2]	1:200/1:1,000[3]	1:1,000	Little *et al.* (2001)
TAG-1	Hybridoma Bank	Mouse IgM, mc[1]	1:150	n.a.	Wolfer *et al.* (1994)
β-Actin	Sigma	Mouse, mc[1]	n.a.	1:10,000	Mulder *et al.* (2011)
β-III-tubulin	Promega	Mouse, mc[1]	n.a.	1:2,000	Keimpema *et al.* (2013)

[1]monoclonal antibody, [2]polyclonal antibody [3]*in vivo/in vitro* dilutions

Supplementary Table II | List of qPCR primers.

Quantitative PCR reactions were performed with primer pairs amplifying short fragments for each gene. Primer pairs were designed to efficiently anneal to homologous nucleotide sequences from mouse and rat. T_A, annealing temperature. Forward and reverse indicate primer orientation.

GenBank Number	Protein	Primer pair[a]	T_A (°C)[b]	Localization
NM_007726	CB1R	(forward) 5'-TCTTAGACGGCCTTGCAGAT-3' (reverse) 5'-AGGGACTACCCCTGAAGGAA-3'	60	Exon2 Exon 2
NM_198114	DAGLα	(forward) 5'-TCATGGAGGGGCTCAATAAG-3' (reverse) 5'-AGCCCTCCAGACTCATCTCA-3'	60	Exon 18 Exon 20
NM_144915	DAGLβ	(forward) 5'-GTGTGCTGTGGTGGATTGTC-3' (reverse) 5'-TCTCATGCTGACACACACGA-3'	60	Exon 1/2 Exon 2
NM_011844	MGL	(forward) 5'-CAGAGAGGCCAACCTACTTTTC-3' (reverse) 5'-ATGCGCCCCAAGGTCATATTT-3'	62	Exon 2/3 Exon 4
NM_019413.2	Robo1	(forward) 5'-GTGATCCCCGATCTCAGAAA-3' (reverse) 5'-GTTGCCAAGTGACCAGGATT-3'	60	Exon 14 Exon 15
NM_175549.4	Robo2	(forward) 5'-GGAGTGGACCACAGACAGGT-3' (reverse) 5'-CCCGAAGTCTGACGGTACAT-3'	60	Exon 13 Exon 14
NM_015748.3	Slit1	(forward) 5'-TCACTGACCTGCAGAACTGG-3' (reverse) 5'-ACCATCTGGTCGAAGGTGAC-3'	60	Exon 32 Exon 34
NM_178804.3	Slit2	(forward) 5'-CGCTGCCTGTCAAACAACTA-3' (reverse) 5'-CGCACTTCACCACTTTCTCA-3'	60	Exon 36 Exon 36
NM_008084	Gapdh	(forward) 5'-AACTTTGGCATTGTGGAAGG-3' (reverse) 5'-ACACATTGGGGGTAGGAACA-3'	60/62	Exon5 Exon7

[a]'forward' and 'reverse' indicate primer orientation
[b]annealing temperature

Supplementary Table III | List of human fetal tissues used for histochemistry.

Characteristics of human fetal tissues used in this study, including their gestational age (weeks + days), sex and cause of death.

Case	gestational age	sex	cause of death
control 1	20 + 5	female	preterm birth
control 2	21 + 2	male	preterm premature rupture of membranes
control 3	22 + 5	male	spontaneous abortion

Supplementary Table IV | CodeSet information for Nanostring Elements.

ACTB: Actin, beta; heat shock protein 90 kDa α (cytosolic), class B member 1; Robo1: roundabout, axon guidance receptor, homolog1; Slit1: slit homolog 1;TBP: TATA box-binding protein; HKG: housekeeping gene.

Accession	Gene ID	Position	Target Sequence	Flags	Tag
NM_001101.2	ACTB	1011-1110	TGCAGAAGGAGATCACTGCCCTGGCACCCAGCACAATGAAGATCAAGATCA TTGCTCCTCCTGAGCGCAAGTACTCCGTGTGGATCGGCGGCTCCATCCT	HKG	T008
NM_007355.2	HSP90ab1	1881-1990	AGCCAATATGGAGCGGATCATGAAAGCCCAGGCACTTCGGGACAACTCC ACCATGGGCTATATGATGGCCAAAAAGCACCTGGAGATCAACCCTGACCAC	HKG	T007
NM_002941.2	Robo1	6396-6495	TGAACCACAAAAAAAAAGGCTGGTGTTCACCAAAACCAAACTTGTTCATT TAGATAATTTGAAAAAGTTCCATAGAAAAGGCGTGCAGTACTAAGGGAAC		T001
NM_003061.2	Slit1	6251-6350	AAGAGGCCCTGAATATACGATTGCCTGCCCACGTTGTCTTCTCTTCCATAC ACAGTGAAAATGTAGAAAGATGGTTTGTGAGGCCAAACTGTGAATGGGC		T003
NM_001172085.1	TBP	588-687	ACAGTGAATCTTGGTTGTAAACTTGACCTAAAGACCATTGCACTTCGTGCC CGAAACGCCGAATATAATCCCAAGCGGTTTGCTGCGGTAATCATGAGGA	HKG	T006

SUPPLEMENTARY REFERENCES

1. Bologa, L., Aizenman, Y., Chiappelli, F., & de, V.J. Regulation of myelin basic protein in oligodendrocytes by a soluble neuronal factor. *J Neurosci. Res.* **15**, 521-528 (1986).
2. Rothberg, J.M., Jacobs, J.R., Goodman, C.S., & Artavanis-Tsakonas, S. slit: an extracellular protein necessary for development of midline glia and commissural axon pathways contains both EGF and LRR domains. *Genes Dev.* **4**, 2169-2187 (1990).
3. Benowitz, L.I. & Routtenberg, A. GAP-43: an intrinsic determinant of neuronal development and plasticity. *Trends Neurosci.* **20**, 84-91 (1997).
4. Kasama-Yoshida, H. *et al.* A comparative study of 2',3'-cyclic-nucleotide 3'-phosphodiesterase in vertebrates: cDNA cloning and amino acid sequences for chicken and bullfrog enzymes. *J Neurochem.* **69**, 1335-1342 (1997).
5. Little, M.H. *et al.* Dual trafficking of Slit3 to mitochondria and cell surface demonstrates novel localization for Slit protein. *Am. J. Physiol Cell Physiol* **281**, C486-C495 (2001).
6. Andrews, W. *et al.* Robo1 regulates the development of major axon tracts and interneuron migration in the forebrain. *Development* **133**, 2243-2252 (2006).
7. Keays, D.A. Neuronal migration: unraveling the molecular pathway with humans, mice, and a fungus. *Mamm. Genome* **18**, 425-430 (2007).
8. Zhao, L., Tian, D., Xia, M., Macklin, W.B., & Feng, Y. Rescuing qkV dysmyelination by a single isoform of the selective RNA-binding protein QKI. *J Neurosci.* **26**, 11278-11286 (2006).
9. Mulder, J. *et al.* Endocannabinoid signaling controls pyramidal cell specification and long-range axon patterning. *Proc. Natl. Acad. Sci. U. S. A* **105**, 8760-8765 (2008).
10. Mulder, J. *et al.* Molecular reorganization of endocannabinoid signalling in Alzheimer's disease. *Brain* **134**, 1041-1060 (2011).
11. Antonucci, F. *et al.* Cracking down on inhibition: selective removal of GABAergic interneurons from hippocampal networks. *J Neurosci.* **32**, 1989-2001 (2012).
12. Lopez-Bendito, G. *et al.* Tangential neuronal migration controls axon guidance: a role for neuregulin-1 in thalamocortical axon navigation. *Cell* **125**, 127-142 (2006).
13. Keimpema, E. *et al.* Nerve growth factor scales endocannabinoid signaling by regulating monoacylglycerol lipase turnover in developing cholinergic neurons. *Proc. Natl. Acad. Sci. U. S. A* **110**, 1935-1940 (2013).
14. Wu, C.S. *et al.* Requirement of cannabinoid CB(1) receptors in cortical pyramidal neurons for appropriate development of corticothalamic and thalamocortical projections. *Eur. J. Neurosci.* **32**, 693-706 (2010).
15. Bekku, Y. & Oohashi, T. Neurocan contributes to the molecular heterogeneity of the perinodal ECM. *Arch. Histol. Cytol.* **73**, 95-102 (2010).
16. Wolfer, D.P., Henehan-Beatty, A., Stoeckli, E.T., Sonderegger, P., & Lipp, H.P. Distribution of TAG-1/axonin-1 in fibre tracts and migratory streams of the developing mouse nervous system. *J. Comp Neurol.* **345**, 1-32 (1994).
17. Tucker, K.L., Meyer, M., & Barde, Y.A. Neurotrophins are required for nerve growth during development. *Nat. Neurosci.* **4**, 29-37 (2001).
18. Berghuis, P. *et al.* Hardwiring the brain: endocannabinoids shape neuronal connectivity. *Science* **316**, 1212-1216 (2007).
19. Molnar, Z. & Blakemore, C. How do thalamic axons find their way to the cortex? *Trends Neurosci.* **18**, 389-397 (1995).
20. Denaxa, M., Chan, C.H., Schachner, M., Parnavelas, J.G., & Karagogeos, D. The adhesion molecule TAG-1 mediates the migration of cortical interneurons from the ganglionic eminence along the corticofugal fiber system. *Development* **128**, 4635-4644 (2001).
21. Ortar, G. *et al.* Tetrahydrolipstatin analogues as modulators of endocannabinoid 2-arachidonoylglycerol metabolism. *J. Med. Chem.* **51**, 6970-6979 (2008).
22. Andrews, W. *et al.* The role of Slit-Robo signaling in the generation, migration and morphological differentiation of cortical interneurons. *Dev. Biol.* **313**, 648-658 (2008).